Table IV
Triad Structures in Copolymers of 2-MOCB and 2-MOCP[a]

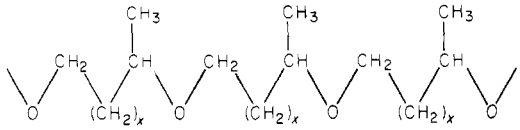

A

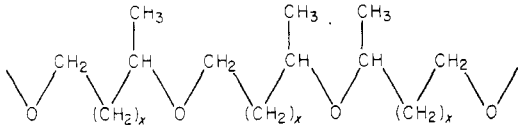

B

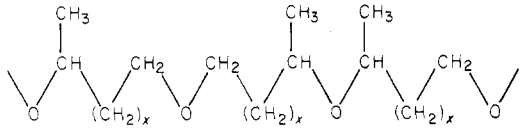

C

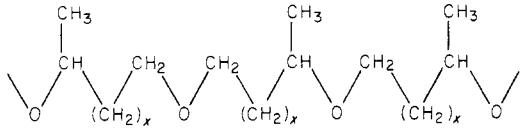

D

[a] $x = 1$ for 2-MOCB units; $x = 2$ for 2-MOCP units.

altered, corresponding to a major signal from the HT units and two signals from the HH units, one of which (signal f) appears to coincide with the large signal from the C-2 in 2-MOCB in the HT configuration around 72.6 ppm. The methylene carbons in 2-MOCP adjacent to oxygen (C-5) give signals that are displaced downfield according to prediction, although to a smaller extent. The fact that two signals are observed with nearly the same separation as for 2-MOCB indicates the formation of TT units. Finally, the other two methylene carbons in 2-MOCP give signals that show upfield shifts, in accordance with prediction, when compared with 2-MOCB.

The values for 2-MOCP in Table II are also in good agreement with the signal positions already given for the diethyl ether of 1,4 pentanediol. In this connection it should be noted that the signal for C-5 in the diethyl ether is in close agreement with the TT signal listed in Table II, in agreement with the structural similarity.

The amounts of 2-MOCP in the copolymers were estimated on the basis of the intensities of the signals from the various carbons relative to those of the reference carbons in the 2-MOCB plus the 2-MOCP units. The values calculated on this basis were 9 and 10% for the copolymers prepared at 0 and −30 °C, respectively. Since both copolymers were prepared from equal molar feed ratios, the reactivity of 2-MOCP is obviously much lower than that of 2-MOCB. The copolymer prepared at lower conversion at 0 °C contained a relatively smaller amount of the less reactive monomer.

Stereoisomerism is not observed for the copolymers under the conditions employed. However, we have previously shown that tacticity may be detected in poly(2-MOCB), particularly when the NMR analysis is performed with a more powerful instrument.[9,10] For the 2-MOCP units, the chiral carbons are in ϵ positions in the HT units and the tacticity effects are expected to be very small, if observable at all.

Registry No. Et_3OPF_6, 17950-40-2; 2-MOCP–2-MOCB copolymer, 86101-64-6.

References and Notes

(1) Chiang, R.; Rhodes, J. H. *J. Polym. Sci., Polym. Lett. Ed.* **1969**, *7*, 643.
(2) Garrido, L.; Guzmán, J.; Riande, E. *Macromolecules* **1981**, *14*, 1132.
(3) Rose, J. B. Ref 6 in "The Chemistry of Cationic Polymerization"; Plesch, P. H., Ed.; Pergamon Press: Oxford, 1963; p 433.
(4) Pruckmayer, G.; Wu, T. K. *Macromolecules* **1973**, *6*, 33.
(5) Tsuda, T.; Nomura, T.; Yamashita, Y. *Makromol. Chem.* **1965**, *86*, 301.
(6) Yamashita, Y.; Tsuda, T.; Okada, M.; Iwatsuki, S. *J. Polym. Sci., Part A-1* **1966**, *4*, 2121.
(7) Tsuda, T.; Yamashita, Y. *Makromol. Chem.* **1966**, *99*, 297.
(8) Malanga, M.; Vogl, O. *J. Polym. Sci., Polym. Chem. Ed.* **1982**, *20*, 2033.
(9) Kops, J.; Hvilsted, S.; Spanggaard, H. *Macromolecules* **1980**, *13*, 1058.
(10) Kops, J.; Spanggaard, H. *Macromolecules* **1982**, *15*, 1200.
(11) Hvilsted, S.; Kops, J. *Macromolecules* **1979**, *12*, 894.
(12) Grant, D. M.; Paul, E. G. *J. Am. Chem. Soc.* **1964**, *86*, 2984.
(13) Lindeman, L. P.; Adams, J. C. *Anal. Chem.* **1971**, *43*, 1245.

On the Radial Structure of Kevlar

S. B. WARNER*

Celanese Research Company, Summit, New Jersey 07901.

Received December 13, 1982

A great deal of activity has appeared in the literature relating to various aspects of the structure of du Pont's commercial lyotropic polymer fiber Kevlar, poly(*p*-phenyleneterephthalamide) (see, for example, ref 1–9). One unique feature of Kevlar, which has been pointed out by Blades,[1] is that Kevlar, unlike most other synthetic fibers, is *not* transversely isotropic. This circularly symmetric birefringence in the crosss section, or lateral birefringence, is extremely difficult to measure;[1] however, it is an important structural feature that seems to be absent from a number of the proposed structural models. In this paper an alternative, simpler technique for assessing lateral birefringence is outlined.

One technique that can be used to examine radial/circumferential structure is interference microscopy, albeit the technique is generally restricted to assessment of skin–core birefringence or thicknesses. Interference microscopy, originally outlined by Faust[10] and used over the years by several microscopists,[11–13] has shown a recent revival[14,15] primarily because it is the basis of a patent claim to Frankfort and Knox[16] on high-speed spinning of poly(ethylene terephthalate) (PET). In this case, the high skin–low core birefringence seems to develop because of the materials' response to temperature gradients along the diameter of the fiber during spinning. The technique, however, can also be employed to assess lateral birefringence under appropriate conditions.

The procedure for obtaining the necessary interference micrographs of fibers consists of immersing a filament in a liquid of refractive index n_L such that the maximum fringe displacement, d_{max}, is about half the fringe spacing, D. Polarizer or analyzer must be oriented appropriately. Three interference micrographs are required (four independent ones are possible) for analysis of $n_{F_\parallel}$ and $n_{F_\perp}$, the indices of refraction of the fiber parallel and normal to the fiber axis, respectively, and t, and the thickness of the fiber, as a function of radial position. The conditions employed in this study are as follows: $n_{L_1} = 1.592 < n_{F_\perp}$ (A in Figures

* Present address: Kimberly-Clark Corp., Neenah, WI 54956.

0024-9297/83/2216-1546$01.50/0

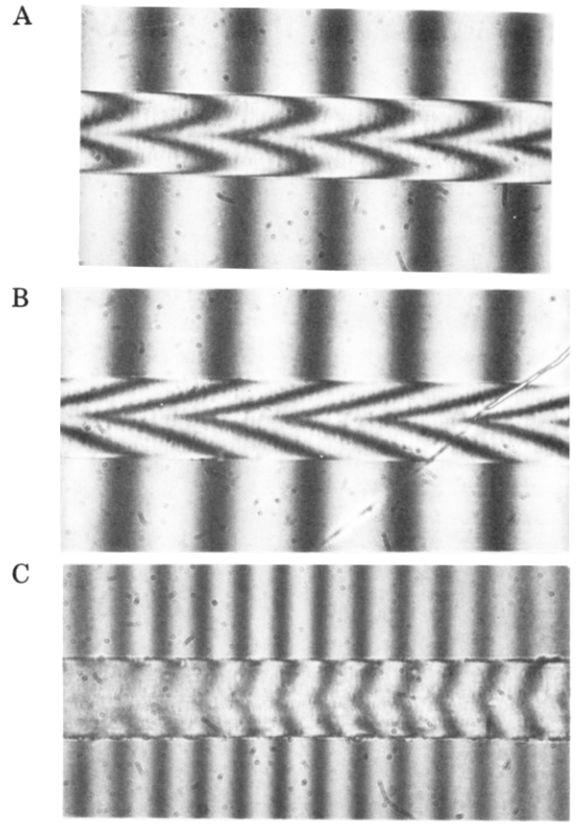

Figure 1. Interference photomicrographs of 2.25-dtex Kevler 29. 1000×, oil. (A) $n_{L_1} = 1.592$ (analyzer perpendicular to fiber axis); (B) $n_{L_2} = 1.632$ (analyzer perpendicular to fiber axis); (C) $n_{L_3} = 2.05$ (analyzer parallel to fiber axis).

1); $n_{L_2} = 1.632 > n_{F_\perp}$ (B in Figures 1); $n_{L_3} = 2.05 < n_{F_\parallel}$ (C in Figures 1); $n_{L_4} > n_{F_\parallel}$ (not used). Photomicrographs were taken at 1000×, oil, using a Leitz Mach-Zehnder double-beam interference microscope and are shown in Figure 1. The data presented in this note are for 2.25-dtex Kevlar 29; however, they are representative of smaller dtex Kevlar 29 as well as Kevlar 49. (dtex, a standard textile term, refers to the weight in grams of 10 000 m of fiber. It is a relative measure of fiber diameter: 2.25-dtex Kevlar has a fiber diameter of about 17 μm.)

Analysis of photomicrographs is facilitated by implementation of the interference equation[16] $d/D = t\,(n_F - n_L)/\lambda$, where d is the fringe displacement and λ is the wavelength of the monochromatic radiation. The equation is solved three times simultaneously for $n_{F\parallel}$, $n_{F\perp}$, and t using the various values of $d_{1\text{-}3}$, $D_{1\text{-}3}$, and $n_{L_{1\text{-}3}}$ at a number of positions along the diameter of a fiber. For this note the information contained in the photomicrographs is graphically input via a digital tablet into a HP 85, where data reduction occurred. Both graphical and tabular data were output, and values every 5% along the diameter were calculated and are shown in Tables I and II. A "shell" analysis[17] is not appropriate for these data.

Typically, fibers are analyzed in this fashion for radial variations in indices of refraction or, so-called skin–core birefringence. PET spun under high-speed conditions and other fibers are characterized by a higher surface than core birefringence.[16] Quantitative analysis proceeds on the assumption that fibers are transversely isotropic, an assumption that is rarely checked! The results of the analysis of Kevlar are shown in Figure 2: birefringence near the surface is about 0.435 and the value at the center is about 0.461. There is no readily envisioned mechanism by which Kevlar might be imparted a *much* higher orientation at the center than at the surface and indeed this is *not* the

Table I
Digitized Interference Data for 2.25-dtex Kevlar 29

dist along fiber diam, %	fringe displacement, (d), nm		
	A	B	C
5	257.3	81.2	155.3
10	337.9	−11.4	164.7
15	366.9	−70.4	139.2
20	375.3	−144.6	114.1
25	357.1	−224.3	91.4
25	357.1	−224.3	91.4
30	306.4	−313.9	70.7
35	218.0	−416.0	49.9
40	141.4	−514.3	30.3
45	62.2	−624.6	10.4
50	−57.6	−740.7	−1.4
45	−16.4	−613.2	−2.9
40	93.2	−514.5	5.3
35	181.5	−435.0	17.4
30	286.2	−318.2	33.4
25	348.9	−236.0	56.3
20	300.7	−159.9	85.2
15	385.6	−93.9	118.5
10	389.2	−19.7	133.4
5	254.8	105.9	126.4

Table II
Radial Variations in Indices of Refraction of 2.25-dtex Kevlar 29

dist along fiber diam, %	$n_\perp$	$n_\parallel$	Δn	thickness of section, μm
5	2.0853	1.6504	0.4349	4.40
10	2.0689	1.6307	0.4382	8.73
15	2.0627	1.6256	0.4371	10.93
20	2.0588	1.6209	0.4379	13.00
25	2.0563	1.6166	0.4397	14.54
30	2.0546	1.6118	0.4428	15.51
35	2.0531	1.6058	0.4473	15.85
40	2.0519	1.6006	0.4513	16.39
45	2.0506	1.5956	0.4550	17.17
50	2.0499	1.5886	0.4613	17.08
45	2.0498	1.5909	0.4589	14.92
40	2.0504	1.5981	0.4523	15.19
35	2.0511	1.6038	0.4473	15.41
30	2.0522	1.6109	0.4413	15.11
25	2.0539	1.6159	0.4380	14.62
20	2.0563	1.6202	0.4361	13.51
15	2.0599	1.6242	0.4357	11.99
10	2.0662	1.6300	0.4362	9.72
5	2.0827	1.6557	0.4270	4.47

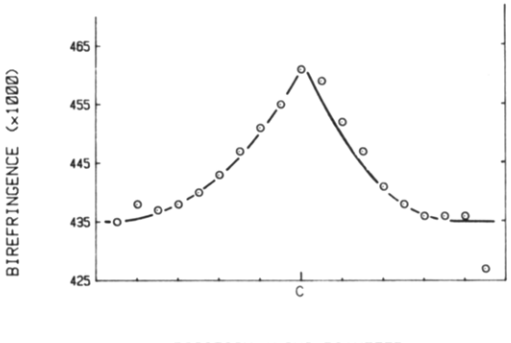

Figure 2. Radial variations in birefringence in 2.25-dtex Kevlar 29.

case. If one assumes that Kevlar has *no* skin–core difference in orientation, then the observed phenomenon is due to *lateral* birefringence; i.e., Kevlar has a radial or circumferential structure. Light rays vibrating perpendicular to the fiber axis that pass close to the surface of the filament (Ā in Figure 3) pass through circumferentially (providing n_c) whereas light rays that pass through the

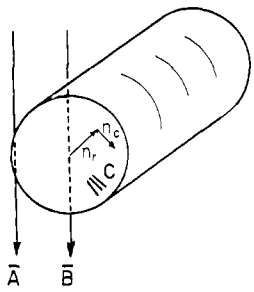

Figure 3. Light ray paths through a fiber.

fiber at the center do so radially ($\bar{B}$ in Figure 3, providing n_r). Thus, the difference in the core–surface birefringence is really the lateral birefringence; i.e.

$$\Delta n_{\text{skin-core}} = (n_{\parallel} - n_{\perp})_{\text{surface}} - (n_{\parallel} - n_{\perp})_{\text{core}} \quad (1)$$

where $n_{\parallel}$ and $n_{\perp}$ refer to indices of refraction relative to the fiber axis. Thus, $\Delta n_{\text{skin-core}}$ is the differential birefringence or the difference in birefringence of the fiber measured at the core or center of the fiber from that measured at the surface. From Figure 3, $n_{\perp_s} \equiv n_c$ and $n_{\perp_c} \equiv n_r$, and

$$\Delta n_{s/c} = (n_{\parallel_s} - n_c) - (n_{\parallel_c} - n_r) \quad (2)$$

Assuming $n_{\parallel}$ does not vary with radial position, that is, the limiting case where all the variation in $\Delta n_{s/c}$ is due to lateral birefringence and none to radial variations in $n_{\parallel}$

$$n_{\parallel_s} = n_{\parallel_c}$$

and

$$\Delta n_{s/c} = n_r - n_c \equiv \Delta n_{\text{lat}} \quad (3)$$

Direct measurements of lateral birefringence of Kevlar have been made[1] and shown $n_r - n_c \geq 0.020$; however, sample preparation for these measurements is extremely difficult. The results here show $n_r - n_c = 0.026$.

Since $n_r > n_c$ in Kevlar, the plane of the aromatic groups lies radially (C in Figure 3) as opposed to circumferentially. This finding is in accord with Dobbs,[8] based on measurements using electron microscopy, and Blades,[1] based on measurements of lateral birefringence.

Registry No. Poly(*p*-phenyleneterephthalamide), 24938-64-5; *p*-phenylenediamine–terephthalic acid, 25035-37-4.

References and Notes

(1) Blades, H. U.S. Patent 3 869 430, 1975.
(2) Pruneda, C. O.; Steele, W. J.; Kershaw, R. P.; Morgan, R. J. *Polym. Prepr., Am. Chem. Soc., Div. Polym. Chem.* **1981**, *22*, 216.
(3) Chapoy, L. L.; Spaseska, D.; Rasmussen, K.; Dupre, D. B. *Macromolecules* **1979**, *12*, 680.
(4) Avakian, P.; Blume, R. C.; Gierke, T. D.; Yang, H. H.; Panar, M. *Polym. Prepr., Am. Chem. Soc., Div. Polym. Chem.* **1980**, *21*, 8.
(5) Simmens, S. C.; Hearle, J. W. S. *J. Polym. Sci., Polym. Phys. Ed.* **1980**, *18*, 871.
(6) Dobb, M. G.; Hindeleh, A. M.; Johnson, D. J.; Saville, B. P. *Nature (London)* **1975**, *253*, 189.
(7) Dobb, M. G.; Johnson, D. J.; Saville, B. P. *J. Polym. Sci., Polym. Symp.* **1977**, *No. 58*, 237.
(8) Dobb, M. G.; Johnson, D. J.; Saville, B. P. *J. Polym. Sci., Polym. Phys. Ed.* **1977**, *15*, 2201.
(9) Dobb, M. G.; Johnson, D. J.; Majeed, A.; Saville, B. P. *Polymer* **1979**, *20*, 1284.
(10) Faust, R. C. *Proc. Phys. Soc. London, Sect. B* **1952**, *65*, 48.
(11) McLean, J. H. *Text. Res. J.* **1971**, *42*, 36.
(12) Scott, R. G. *Sci. Tech. Inf.* **1971**, *2*, 36.
(13) Barakat, N.; El-Hennawi, H. A. *Text. Res. J.* **1971**, *42*, 391.
(14) Perex, O.; LeCluse, C. *Int. Chem. Dornbirn* **1979**, *20*, 1.
(15) Hamza, A. A.; Fouda, I. M.; El-Farhatg, K. A.; Badawy, Y. K. *Text. Res. J.* **1980**, *51*, 592.
(16) Frankfort, H.; Knox, B. U.S. Patent 4 134 882, 1979.
(17) Kuhnle, G.; Schollmeyer, E.; Herlinger, H. *Makromol. Chem.* **1977**, *178*, 2725.

Theory of α-Helix-to-Random-Coil Transitions of Two-Chain, Coiled Coils. Application to the T1 and T2 Fragments of α-Tropomyosin

JEFFREY SKOLNICK and ALFRED HOLTZER*

Department of Chemistry, Washington University, St. Louis, Missouri 63130. *Received February 16, 1983*

In previous papers in this series, an equilibrium statistical mechanical theory is developed and used to fit data for the thermally induced α-helix-to-random-coil transition of two-chain, coiled coils.[1-4] In that work, application of the theory is made to cross-linked and non-cross-linked α-tropomyosin at both near-neutral[3] and acidic pH[4] and to a synthetic 43-residue peptide made to model salient features of the α-tropomyosin amino acid sequence.[2,5]

This theory requires as input the amino acid sequence of the polypeptide chain in question and appropriate values, for each amino acid type, of the parameters governing the "short-range" interactions, i.e., the helix initiation (σ) and propagation ($s(T)$) parameters.[6] The sequence of α-tropomyosin is available.[7] Algorithms were developed[4,5] for obtaining $s(T)$ values that reproduce the measurements of that quantity.[8] Values of σ can be obtained from the same source.[8] The theory also requires measurements of α-helix content at a known protein concentration. This need was supplied from extant or newly generated circular dichroism data. Recently, the formalism has been extended to include effects of loop entropy, but no data have as yet been treated by this more elaborate theory.[9]

With this input information, the theory, as employed thus far, provides a quantity $-RT \ln w^0$ as a function of temperature.[10] The physical significance of $-RT \ln w^0$ is that it represents Avogadro's number times the change in standard free energy when two widely separated, translationally fixed, α-helical blocks are brought together to form the coiled coil.[1] Thus, it measures the helix–helix interaction in the coiled coil.

Thus far, the theory, although it seems to fit the data, has been employed in a relatively crude manner in that it has been assumed that the value of w^0 depends only on temperature and not on the location of the block within the chain.[1-4] This use of a site-independent w^0 is suspect since evidence exists from studies of excised fragments of α-tropomyosin that the half of the molecule near the amino end is more stable than near the carboxyl end.[11-13]

We report here the results of an investigation of possible site dependence of the helix–helix interaction by application of the theory to two fragments of tropomyosin, T1 and T2.[11] These were chosen as particularly apt for our purpose for several reasons: (1) Appropriate thermal denaturation curves, i.e., circular dichroism (usually expressed as mean residue ellipticity [Θ]) vs. T, are available and were determined in the same laboratory, which diminishes systematic errors. (2) These two fragments add up to a full tropomyosin molecule but have no residues in common; i.e., they are obtained from the parent chain by a single cut. (3) The cut is almost in the middle of the chain so that each fragment has about the same degree of polymerization. This ensures that certain statistical effects due to chain length are not the source of any observed differences. (4) The stabilities of the T1 and T2 fragments have not been reported to be dependent on the method of isolation, as is the case for some other fragments.[11]

It will be seen that the theory allows us to compare the two halves of the tropomyosin polypeptide chain with respect to the helix-promoting influence of both the "short-range" interactions and the "long-range" (i.e., helix–helix) interactions.

0024-9297/83/2216-1548$01.50/0